Development of "Sweet" Soy-Based, High Biorenewable Content UV-Curable Coatings

**By Zhigang Chen,
Jennifer F. Wu,
Shashi Fernando and
Katie Jagodzinski**

The fast depleting petroleum reserve and the ever-increasing cost is attracting even more serious attention to the industrial utilization of biorenewable raw materials in the chemical industry.[1,2] Organic coatings are an important sector of the modern chemical industry. However, traditional coatings contain a significant amount of organic solvents and other volatiles. The coatings industry has been identified as second only to the gasoline-automobile complex as the largest source of the volatile organic compound (VOC) pollutants that are responsible for excess ozone in the air.[3]

Driven by the rising raw material cost and the stricter environmental regulations, the coatings industry is transforming into a "greener" industry by incorporating more alternative renewable raw materials and cleaner technologies such as radiation cure, high solids and waterborne coating technologies.[4,5] Radiation-cure coating technology—including ultraviolet (UV) and electron beam (EB) cure—is a green coating technology that has the capability to produce high-performance coatings with high productivity, low-energy consumption and extremely low VOC emissions.[6-8] It has been enjoying fast market growth since its introduction to the coatings industry.[5,9] Utilization

of biorenewable raw materials in radiation-cure coatings is a promising "green+green" solution to the challenges facing the industry.

Bio-derived chemicals such as drying oils have a long history of being used as coating ingredients. Bio-derived chemicals have appealing features, including being environmentally benign and exhibiting short regeneration cycles which meet the demand of a sustainable chemical industry.[2] On the other hand, quality control, land uses and logistic costs are potential issues in the industrial utilization of bio-derived chemicals. The intense research and development in the petroleum-based chemical industry that has been ongoing since the early 20th century has been providing the coatings industry with very cost-effective, high-quality raw materials. Thus, one major challenge in generating bio-based materials in order to substitute for their petrochemical-based counterparts is to match or even surpass the performance of petrochemical-based materials with competitive cost.

Blending bio-derived ingredients into existing petrochemical-based formulations is an intuitive approach to utilize bio-derived chemicals. However, normally lower biorenewable content materials are produced in order to

maintain the material performance, despite the fact that coating materials with high biorenewable content are highly desired.

An alternative approach to obtain high-biorenewable content, high-performance materials is to custom design and formulate the resin and coating system according to specific application needs based on the understanding of the structure-property relationships of bio-derived chemicals. With this approach, it is expected that the structural features and the related material properties of the bio-derived ingredients can be fully utilized in the formulations to achieve optimal material performance. At the same time, due to the limited availability of biorenewable raw materials on the current market, use of petrochemicals in formulations is inevitable.

These petrochemicals and their addition should be carefully examined in order to maximize their effect with the lowest loading level. In addition to material performance, there are other important aspects to consider and explore in the development of high biorenewable-content, bio-based materials. For example, it is desirable that the bio-based materials disintegrate in the environment after use via mechanisms (such as microorganism-induced anaerobic or aerobic degradation) without releasing harmful fragments.[10] Consequently, the degradation of these materials and the subsequent tracking and analysis of the released compounds are important research topics. On the other hand, from an application standpoint, the bio-based materials must possess high enough durability throughout their service lifetime to withstand erosion in their service environment (such as microorganism-induced deterioration, hydrolysis and weathering, etc.). These aspects are critical research topics in addition to formulation and performance

enhancement of high biorenewable content, bio-based materials.

Soybean is a major produce in the U.S.[11] Soybean oil-derived chemicals are important biorenewable materials in the coatings industry.[12,13] Acrylated soybean oil (ASO) and epoxidized soybean oil (ESO) have been formulated into UV coatings, but petrochemicals had to be incorporated into ASO or ESO in order to achieve better coating performance.[14-17] Thus, the biorenewable content was lower in these formulations. The softness of the fatty acid triglyceride backbone, and the lower reactivity for the mid-chain functional groups (such as epoxies and acrylates) are the main reasons for the inferior coating film properties.[18,19]

In order to develop soy-based, high-performance, UV-curable coatings with high biorenewable content, the incorporation of highly effective petroleum-based crosslinkers, biorenewable tougheners and reactive diluents into ASO was conducted in this work. Commercial hyperbranched acrylates (HBAs) were selected as the petroleum-based crosslinkers to co-photopolymerize with ASO. To our best knowledge, the use of highly functional hyperbranched acrylates in soy-based, UV-curable materials has not been reported. Owing to their unique branched molecular structures, hyperbranched acrylates exhibit low viscosity, high molecular weight and functionality, and lower photopolymerization shrinkage[20] that are expected to significantly increase the properties of the UV-curable, soy-based formulations.

As to the bio-based toughening monomers and reactive diluents, the "sweet" acrylated sucrose (AS) with varying acrylate functionality and acrylated tetrahydrofurfural (ATHF) were selected. Sucrose (chemical structure shown in Figure 1), commonly known as table sugar, is

an abundant low-cost, biorenewable resource in U.S. The sucrose molecule possesses aliphatic ring structure and multiple hydroxyl groups. The aliphatic ring structure imparts balanced hardness and flexibility to the material, while the hydroxyl groups provide sites for chemical modification and intermolecular hydrogen bonding. AS can be synthesized through various routes, including transesterification with methyl acrylates and methyl methacrylates.[21,22] But the effect of AS as a toughening ingredient in UV-curable coatings has not been investigated despite the idea that the unique molecular structure of AS may significantly alter the soy-based UV-cured coating properties.

Acrylated soybean oil has high viscosity, thus reactive diluents are necessary to lower the viscosity of ASO-based coating formulations. ATHF (structure shown in Figure 1B) is a derivative of furfural alcohol, a bio-derived chemical from a variety of agricultural by-products, including corncobs, oat, wheat bran, sugarcane bagasse and sawdust.[23] ATHF has ~70% biorenewable content, and has low viscosity and high solvency toward common acrylate oligomers and monomers. It is an ideal biorenewable reactive diluent for high biorenewable content, soy-based coating formulations. The research progress toward the production of high-performance and high-biorenewable content, soy-based UV-curable coatings by incorporation of HBAs, ATHF and the "sweet" acrylated sucrose is discussed in this contribution.

Experimental

Materials: Powderized sucrose was purchased from a local grocery store. Methyl acrylate, potassium carbonate, tetrabutylammonium hydroxide, hydroquinone and phenothiazine were purchased from Aldrich. Ebecryl® 860 (ASO-acrylated soybean oil, 3.4 acrylate group per soybean oil molecule),

FIGURE 1

Chemical structure of (A) sucrose and (B) acrylated tetrahydrofurfuryl alcohol

A.   B.
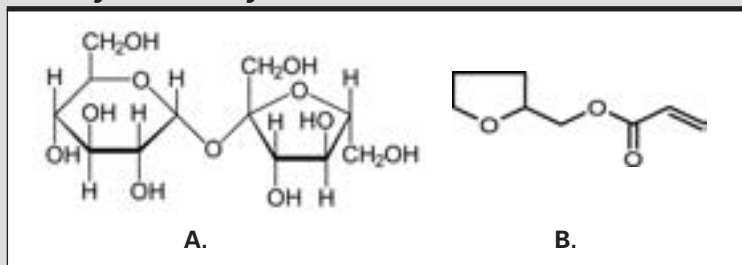
Ebecryl® 168 and Ebecryl® 170 (UV-curable phosphated acrylate adhesion promoter on metal) were supplied by Cytec Industries Inc. Hyperbranched polyester acrylates CN2300 and CN2304 (abbreviated as A8 and A18 respectively, specifications shown in Table 1), and SR285, tetrahydrofurfural, were supplied by Sartomer Company Inc. Irgacure 2022 (PI), a 1:4 by weight photoinitiator blend of Phenylbis(2,4,6-trimethylbenzoyl)-phosphine oxide) and 2-Hydroxy-2-methyl-1-phenyl-1-propanone, was supplied by Ciba Specialty Chemicals.

Synthesis and characterization of acrylated sucrose and methacrylated sucrose (MAS): The AS and MAS were synthesized in bulk following slightly modified procedures based on the procedures described in the literature.[21] A typical procedure for the synthesis of acrylated sucrose is powderized sucrose and tetrabutylammonium hydroxide dried under 50°C in a vacuum oven overnight to remove water. 39.12g sucrose was added into a 250 ml two-neck round-bottom flask containing a Teflon-coated stir bar. Separately, 236.13g methyl acrylate (three times in excess to sucrose), 1.38g potassium carbonate, 2.75g tetrabutylammonium hydroxide, 0.14g hydroquinone and 0.14g phenothiazine were pre-mixed in a beaker and added to the sucrose in the flask.

The flask was connected to a condenser on one neck. A long needle was inserted into the flask through a rubber septum for dry air bubbling on the other neck. The reaction started by heating the flask in a silicone oil bath at 70°C. After a designated reaction time, the reaction product mixture was diluted with acetone and the acrylated products were separated from the unreacted sucrose using vacuum filtration and acetone washing. The acrylated sucrose was recovered by removing acetone and excess methyl acrylate using rotary vacuum evaporation. The IR spectra were recorded with Thermo Scientific Nicolet 8700 Fourier Transform Infrared Spectrometer with detector type DTGS KBr. The mass spectra were obtained with an Applied Biosciences 4000 Q-Trap MS-MS equipped with a turbospray ion source.

UV-curable coating formulation and characterization: The liquid coating formulation was simply prepared by adding and mixing all the ingredients in a vial, and gentle heating was used to help dissolution of the ingredients, if necessary. For coating physical property tests, the liquid coatings were cast on aluminum Q-panels with a wire-wound drawdown rod to form a thin film with ~100 μm thickness, followed by UV curing using a Fusion LC6B Benchtop Conveyor with an F300 UVA lamp (UVA, irradiance ~1548 mW/cm², 2205/cm² measured by UV Power Puck® II from EIT Inc.) in air. Typical curing protocol is one pass through the lamp with a conveyor belt speed of 10 feet/min. The coatings were tested after being conditioned in ambient laboratory conditions for at least 24 hours.

An automated surface energy measurement unit manufactured by Symyx Discovery Tools, Inc. and First Ten Angstroms was used to measure water contact angle on UV-cured, thin-film materials. Three drops of water were used for each measurement, and

TABLE 1

Properties of hyperbranched polyester acrylates

Trade name	Abbreviation	Acrylate functionality	Acrylate equivalent weight (g/mol)	Surface Tension (mN/m @ 25°C)	DMA Tg (°C)
CN2300	A8	8	163	32.6	96
CN2304	A18	18	96	32.6	181

Courtesy of Sartomer Company Inc.

the average contact angle and standard deviation were reported. Hardness testing was performed with a BYK Gardner pendulum hardness tester in König mode; the hardness was reported in seconds. Methyl ethyl ketone (MEK) double rubs were used to assess the solvent resistance of the cured coatings. A 26-ounce hammer with five layers of cheesecloth wrapped around the hammerhead was soaked in MEK for rubbing. The number of double rubs taken to expose the substrate were recorded and reported.

Falling weight direct impact testing was carried out according to ASTM D2794 with a 2-pound weight. The starting height was increased until the film was damaged and/or delaminated from the substrate, and the maximum height at which the film was intact was recorded. Tensile tests were performed using an Instron 5542 testing system (Instron Corp., Norwood, Mass.). ASTM D412-D dumbbell specimens were used. The strain rate was 0.2% s^{-1}. Dynamic mechanical thermal analysis (DMTA) was performed using a TA Instruments Q800 DMA in rectangular tension/compression geometry. The analysis was carried out from -50ºC to 200ºC at a frequency of 1 Hz and a ramp rate of 3ºC min^{-1}. Tg was obtained from the maximum peak in the tan δ curves. Crosslink density (v_e) was calculated according to the equation E'=3v_eRT, where E' value was determined in the linear portion at least 50ºC greater than the Tg. DSC experiments were performed utilizing a TA Instruments Q1000 DSC with a heat-cool-heat cycle. The sample size was ~5.0mg. Temperature was ramped from -50ºC to 200ºC at 10ºC min^{-1} in nitrogen.

Results and Discussion

Synthesis and characterization of acrylated sucrose and methacrylated sucrose: The synthesized acrylated and methacrylated sucrose (AS and MAS)

FIGURE 2

IR spectrum of AS6h showing the appearance of acrylate peaks at 1635 and 807 cm^{-1}
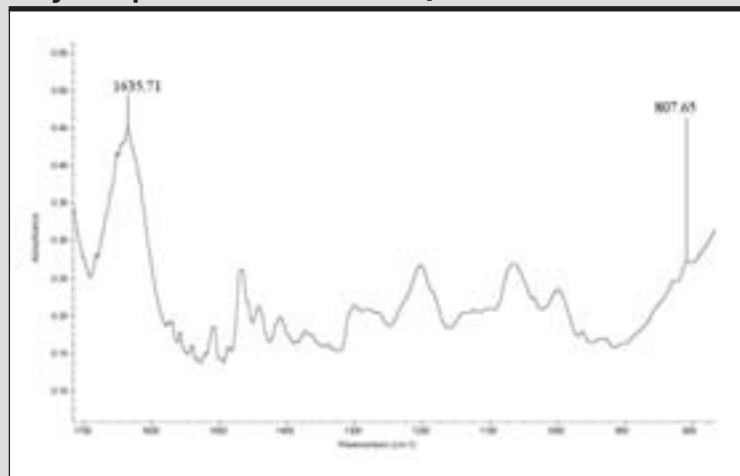
are brown, highly viscous semi-solid materials. Unlike sucrose, which has poor solubility in most organic solvents, the AS and MAS exhibited good solubility in common organic solvents such as acetone, methanol, THF, etc., as well as water. In addition, the AS and MAS showed good solubility in the reactive diluent ATHF. Generally, it was found that AS and MAS products obtained after longer reaction time had better solubility. FTIR and Mass Spectroscopy were used to characterize the synthesized AS and MAS. Figure 2 shows the FTIR spectrum of AS obtained after a 6-hour reaction (AS6h) as an example.

The appearance of the characteristic acrylate peaks at 807 and 1635cm^{-1} indicates the attachment of acrylate group to the sucrose. Figures 3A and 3B show the mass spectra of AS obtained after 6-hour and 12-hour reactions (AS6h and AS12h), respectively. Table 2 lists the theoretical molecular weight calculation for acrylated sucrose with increasing acrylate functionalities. Molecular ion peaks with close molecular weight numbers shown in Table 2 were identified in the mass

spectra for AS6h and AS12h, indicating the existence of AS with a varying degree of acrylation in the product mixture. Also, it was noticed from Figures 3A and 3B that the acrylate functionality of the AS increased with increasing reaction time. In AS6h, five, six and seven acrylate functionalized sucrose oligomers were predominant; in AS12h, seven and eight acrylate functionalized sucrose oligomers were predominant. The Mass Spectroscopy results of AS6h and AS12h showed that the degree and distribution of acrylate functionality of the synthesized AS can be controlled by reaction time. Preliminary UV curing of synthesized AS and MAS were carried out. MAS exhibited poor photopolymerization reactivity, consequently only AS was chosen for formulation study.

Formulation and characterization of soy-based, UV-curable coatings containing acrylated sucrose and hyperbranched acrylates: ASO is a highly viscous liquid. It can be UV cured in seconds by adding 3% wt. PI, but the formulation viscosity is too high for coatings applications. 20% wt. ATHF was added to the ASO and PI blend to

FIGURE 3

Mass spectrum of (A) AS6h and (B) AS12h

(A)

(B)
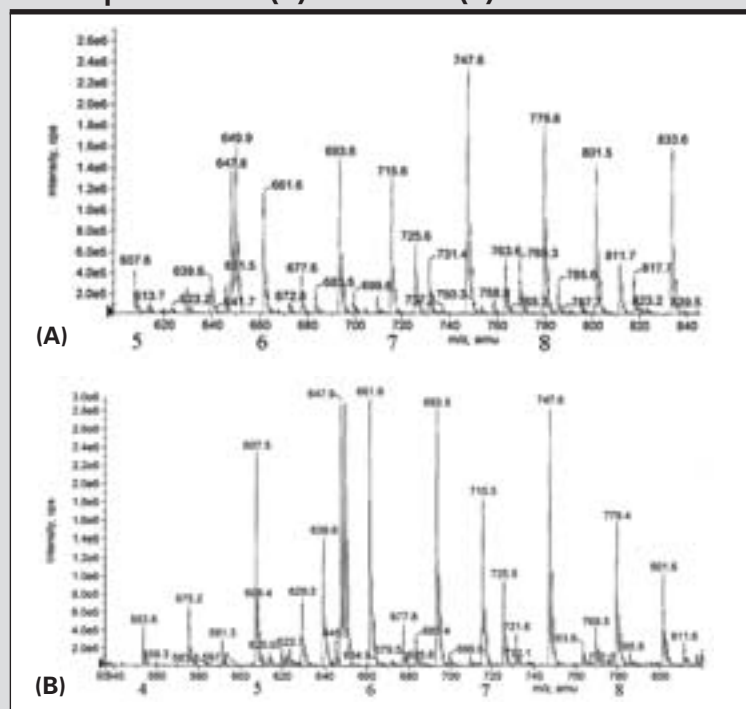
achieve a reference formulation (base) with applicable viscosity. To study the effect of AS and HBAs on the soy-based, UV-curable formulations, AS6h and AS12h, and A8 and A18 were added into the base formulation, together with 5% wt. 1:1 blend of Ebecryl® 168 and 170 for adhesion enhancement on aluminum panels. The coating material performance of these formulations were tested and compared. The coating

physical properties were first tested. Figures 4, 5, 6 and 7 show and compare the coating pendulum hardness, cross-hatch adhesion, impact resistance and solvent resistance, respectively.

Compared to the base formulation, the addition of only 10% wt. HBAs significantly increased the coating hardness and solvent resistance. This enhancement is attributed to the incorporation of higher molecular

weight, multifunctional crosslinkers (HBAs) with higher glass transition temperatures and more rigid polyester backbones in the crosslinked ASO-based coating films. The base formulation has very poor adhesion on aluminum. Upon addition of HBAs and adhesion promoters, the coatings' adhesion was improved. The lower photopolymerization shrinkage of HBAs,[20] the acidic etching of the metal substrate by the adhesion promoters, and the phosphonate complex formation between the metal and the adhesion promoters[24] were attributed to the improved adhesion. The addition of A8 didn't affect the coating impact resistance. On the other hand, the A18 addition increased the impact resistance from 25 inches to 35 inches. The coating impact resistance is an overall evaluation of the coating adhesion, flexibility and toughness. The addition of more rigid A8 and A18 enhanced the coating adhesion due to lower photopolymerization shrinkage; however, the film flexibility didn't increase accordingly, which resulted in only a slight increase in impact resistance.

In contrast to HBAs, the incorporation of 20% wt. AS6h and AS12h into the base formulation generated more durable coating films, as evidenced by the more enhanced coating impact resistance. At the same

TABLE 2

Molecular weight calculation for acrylated sucrose oligomers

Acrylate Functionality	Theoretical MW of AS	+17 (HO⁻)	+23 (Na⁺, from the container glass etc.)
4	558.5	575.5	581.5
5	612.5	629.5	635.5
6	666.5	683.5	689.5
7	720.6	737.6	743.6
8	774.6	791.6	797.6

FIGURE 4

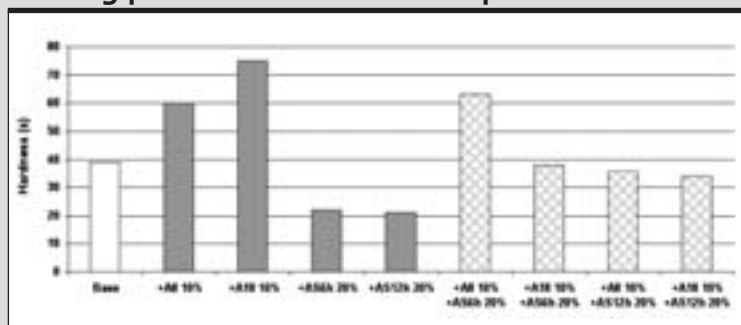### Coating pendulum hardness comparison

FIGURE 5

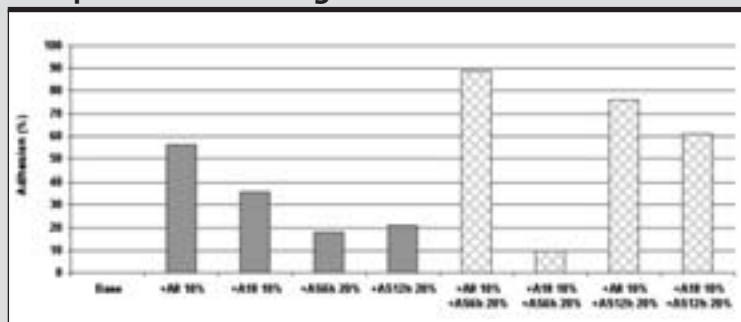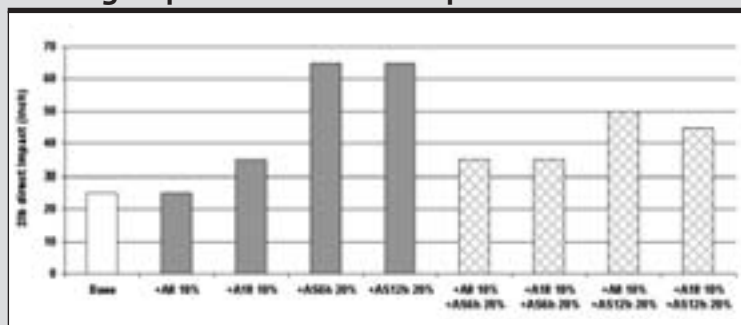### Comparison of coating adhesion to aluminum

FIGURE 6

Coating impact resistance comparison

time, decreased coating hardness and similar solvent resistance were found for the AS-added formulations as compared to the base formulation. These observations suggested that the AS6h and AS12h were acting as reactive flexibilizers in the soy-based coating formulations. Unmodified sucrose molecules have intensive intermolecular hydrogen bonding that results in hard, crystalline material.[25] Upon acrylation, as in the case of AS6h and AS12h, most of the hydroxyls in the sucrose were transformed into photoreactive acrylate groups. Thus, hydrogen bonding in the AS was expected to be less intense. On the other hand, the five- and six-member aliphatic rings connected via an ether bond in the sucrose molecule possess balanced rigidity and flexibility. It can be predicted that a crosslink network with such molecules would afford larger deformation via breaking of the hydrogen bonding and transformation of the acrylated sucrose molecule configuration under external forces before fracturing. Consequently, lower pendulum hardness but tougher coating films with much higher impact resistance were observed with AS addition. Negligible adhesion enhancement was found for the AS-added samples. It is most probably due to the lower molecular weight of the AS molecules as compared to the HBAs, thus the photopolymerization-induced shrinkage is still significantly high enough to affect the adhesion.[20]

The combination of 10% wt. HBAs and 20% wt. AS6h or AS12h into the ASO-based formulations generated balanced coating performance. The coating hardness and impact resistance were in between the properties obtained by adding either the HBA or AS individually. However, it was noticed that the coating solvent resistance was not sacrificed and remained at over 400 double rubs even upon the addition of 20% wt. AS. Also, the coating adhesion for formulations with both HBAs and AS was higher than the formulations with either the HBAs or the AS individual addition, except for the formulation with 10% A18 and 20% AS12h. A synergistic effect between the HBAs and the AS seems to be present—the reactive nature of the AS helps to maintain the excellent solvent resistance obtained by the addition of HBAs, while the relatively flexible AS may contribute to stress dissipation inside the coating during photopolymerization, leading to further

FIGURE 7

Coating solvent resistance comparison
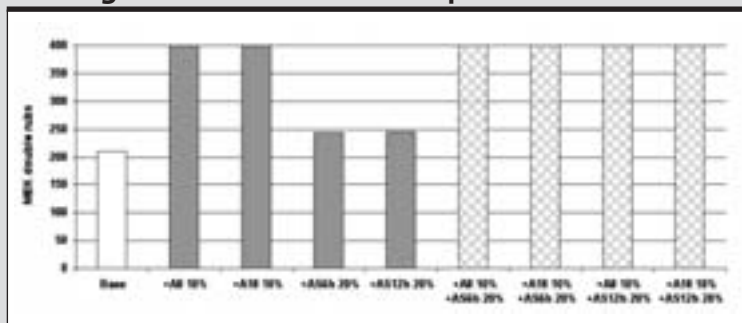
enhanced adhesion after addition of HBAs. This synergistic effect will be further discussed when examining the coating thermal mechanical behavior.

The synthesized AS6h and AS12h had good solubility in water. The effect of their hydrophilicity on the coating surface and bulk properties were evaluated by water contact angle measurements and a water immersion test. Figure 8 shows that the coating produced from the base formulation, which has over 75% wt. ASO, is hydrophobic with a contact angle more than 95 degrees due to the hydrophobic nature of the crosslinked ASO network. Upon addition of HBAs, the coating contact angle decreased to around 85 degrees, as a result of diluting the hydrophobic ASO network with relatively more hydrophilic polyester HBAs. When 20% wt. hydrophilic AS6h or AS12h was added, respectively, into the base formulation, further decrement of the water contact angle was noticed, especially for the formulations containing AS6h, (which is more hydrophilic due to the existence of a higher number of residual hydroxyls). The combination of both HBAs and AS with ASO produced relatively hydrophilic coatings with water contact angles around 80 degrees.

A tap water immersion test was conducted to examine the stability of

AS-added, ASO-based coating films in water—10% or 20% wt. AS6h and AS12h were added to the base formulation together with 10% wt. of A8 or A18. The formulations were applied onto bare aluminum panels, UV-cured and immersed in water for up to seven days. Visual examinations of the coating films were conducted to evaluate the coating film stability in water. Figure 9 shows the images of the coating films taken after seven days water immersion. For the coatings containing 20% wt. either AS6h or AS12h, the films delaminated from the bare aluminum panels after about 24 hours immersion.

The stress generated from coating-film swelling upon water absorption, and the reduced adhesion at the coating-substrate interface due to the

replacement of water[26] were considered the major reasons for the quick delamination from the bare aluminum substrate. This observation confirms the high hydrophilicity of the coatings with high AS loading (20% wt.). With 10% wt. AS6h and AS12h addition, the ASO-based coating films showed rather good stability in water after seven days, as shown in Figure 9. All the other coating films adhered well to the bare aluminum panel, except for the formulation containing 10% wt. AS6h and 10% wt. A8, which showed slight delamination after seven days. Most parts of the immersed coating films remained smooth, while certain spots on the clear films turned hazy due to water absorption. Generally, formulations containing 10% wt. AS6h had relatively lower resistance to water immersion versus the ones containing 10% wt. AS12h, which can be attributed to the higher -OH content in AS6h.

The tensile modulus and elongation at break of the UV-cured, soy-based coating films were obtained and the results shown in Figure 10. Compared to the base formulation, a significant coating modulus increment was achieved upon the addition of HBAs, especially for the coatings containing A18, which has higher acrylate functionality and glass transition temperature than A8. The rigidity of the coating film increased accordingly

FIGURE 8

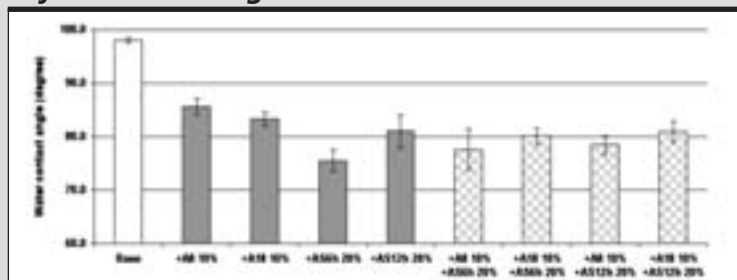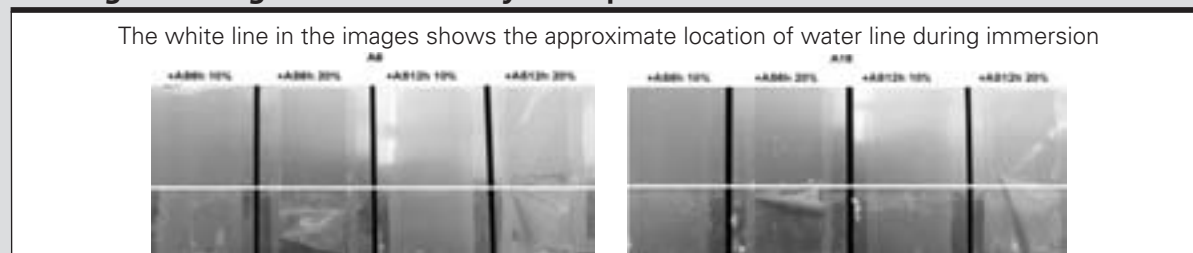**Water contact angle data for UV-cured, soy-based coatings**

FIGURE 9

Coating film images after seven days of tap water immersion

The white line in the images shows the approximate location of water line during immersion


as indicated by the lower elongation at break with the A18 addition. When AS6h or AS12h was added to the base formulation, the film modulus didn't change significantly, but the elongation at break increased by more than 100%. The much enhanced elongation at break value is consistent with the observed much higher impact resistance upon AS addition, demonstrating the significant toughening effect of the AS in the UV-cured, soy-based coatings. A "mixing" effect was noticed for the formulations containing both AS and HBAs, as their modulus and elongation at break data were between the ones with only AS or HBA addition, showing balanced coating mechanical properties.

The glass transition temperature and crosslink density of the soy-based coatings were obtained and calculated from DMTA as shown in Figure 11, and the overlap of the DMTA tanδ curves is shown in Figure 12. The glass transition temperature of the base formulation is around 20°C as a result of the softer, more flexible fatty acid triglyceride backbone of ASO. The polyester HBAs A8 and A18 have much higher glass transition temperatures than ASO due to the more rigid polyester backbone, higher molecular weight and higher acrylate functionality. Upon individual A8 and A18 addition, the main glass transition temperature of the coatings increased to 25-30°C. In addition, the glass transition peak broadened and

FIGURE 10

Tensile modulus and elongation for UV-cured, soy-based coatings
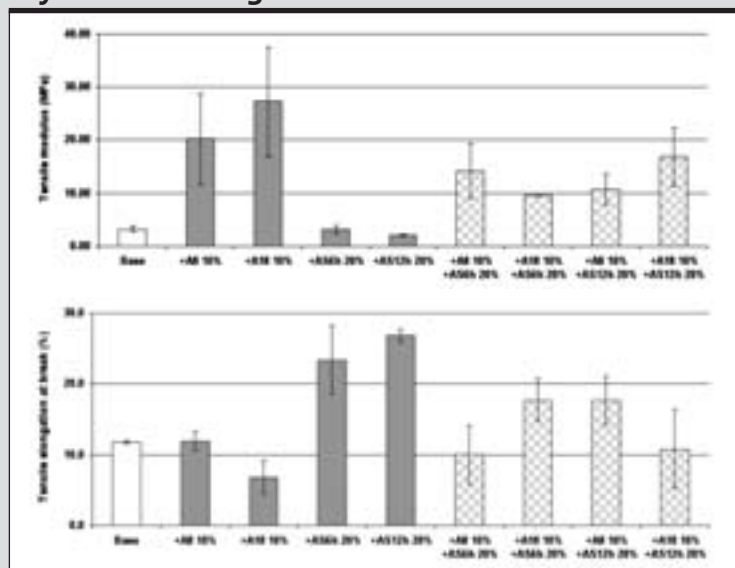
extended to higher temperatures. The higher and broader glass transition in the two HBA-added, UV-cured coating formulations contributed to the higher hardness and modulus of the coatings films, indicating tougher crosslinked network formation. However, the crosslinking density for the two HBA-added formulations (+A8 10% and +A18 10%) were lower than the base formulation.

The earlier photopolymerization-induced vitrification of the higher functionality and higher molecular

weight HBAs-added formulations were considered the reasons for lower crosslink density.[20,27] When only 20% wt. AS6h or AS12h was added to the base formulation, it was noticed from Figures 11 and 12 that the main glass transition of the crosslink network for these two samples didn't change significantly as compared to the base formulation. However, a second transition appears as a shoulder peak of the main transition at higher temperature (about 80°C). The second transition was attributed to the acrylated sucrose in the soy-

FIGURE 11

DMTA glass transition (main) and crosslink density for UV-cured, soy-based coatings
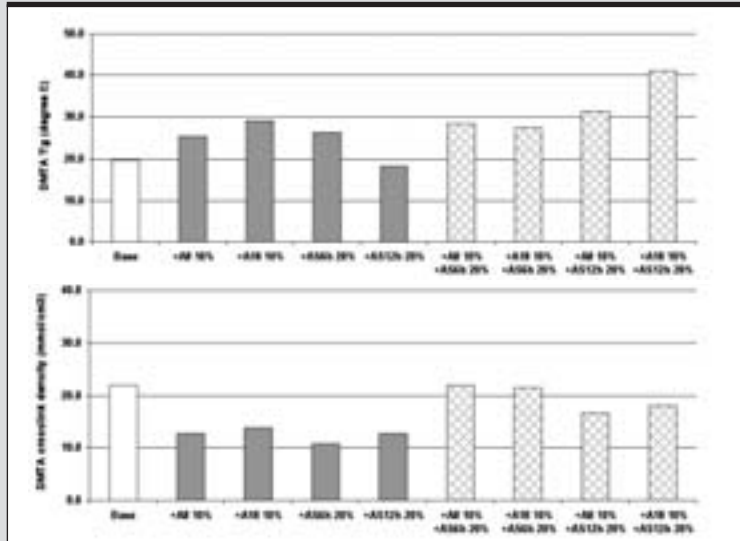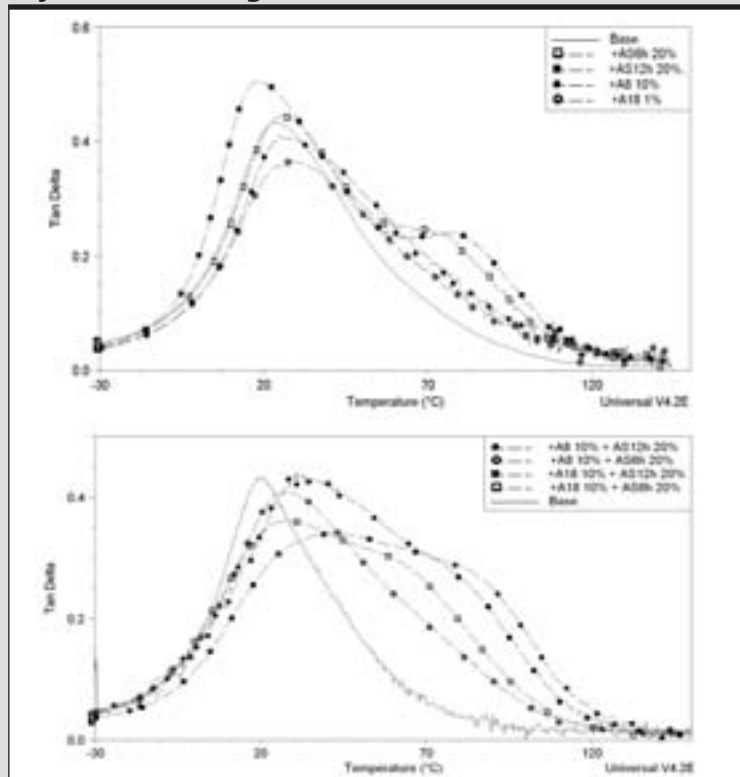

FIGURE 12

**Overlap of DMTA tanδ curves for UV-cured, soy-based coatings**

based, crosslinked coating network. The two transition peaks in the tanδ curves indicates that there are two microphases[28,29] in the crosslinked, acrylated sucrose-added, UV-cured coating films. The predominant phase is the crosslinked ASO, the second phase is the crosslinked acrylated sucrose oligomers.

Due to the more rigid AS ring structure and intermolecular hydrogen bonding, the second phase has higher transition temperature. Since the second transition appears as a shoulder peak of the main transition peak in the tanδ curves, it can be concluded that there is a certain degree of compatibility or "phase mixing" between the ASO and AS phases,[30] largely owing to the chemical bonding formed between ASO and AS during the photopolymerization of the acrylate groups. The presence of two interconnected soft and hard microphases resembles the microphase separation in a typical polyurethane polymer, which exhibits excellent mechanical properties.[30,31] The existence of microphase separation in the AS-added, ASO-based crosslinked network explains in microscopic scale the observed significantly enhanced coating film impact resistance and tensile elongation at break. When both HBAs and AS were added into the ASO-based formulation, it was first noticed from the tanδ curves that the main transition peaks still appear at higher temperatures and are broader than the base formulation, but the higher temperature transition peaks assigned to the AS phase were less distinct, indicating better compatibility between the ASO and AS.

Hyperbranched polymers, owing to their hyperbranched molecular structure, have higher solubility and compatibility with other chemicals.[32,33] Thus, the less distinct higher transition temperature peak is most probably due to the compatibilizer role the HBAs played in the ASO- and AS-added formulations.

FIGURE 13

TGA weight loss curves
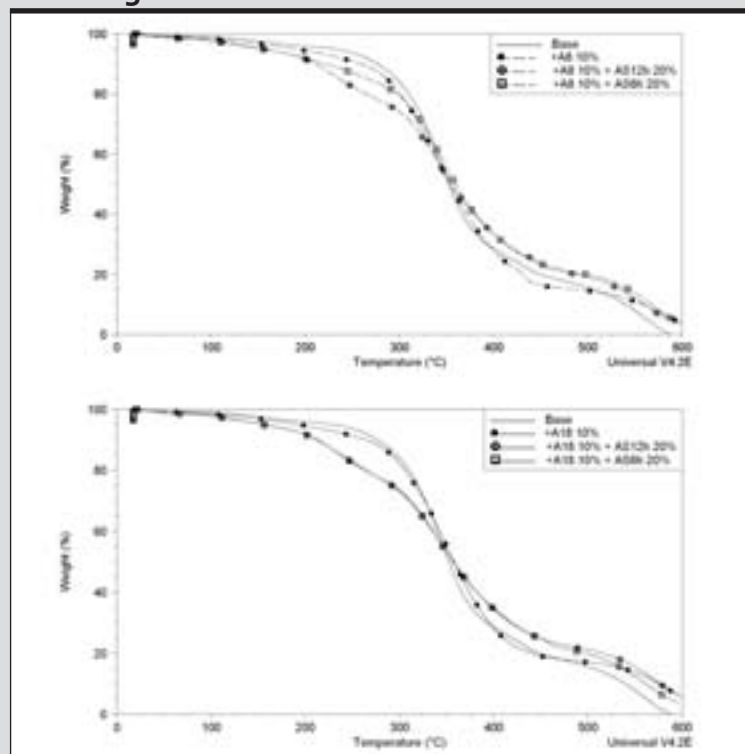
Despite improved compatibility, the less distinct microphase separation and the incorporation of more rigid, higher glass transition temperature HBAs generated coating films with lower impact resistance than the ones with only the AS addition. With regard to other coating film properties (such as tensile modulus and elongation, hardness and impact resistance, etc.), a "mixing effect" was noticed that gives balanced coating properties. Higher crosslink density was found for both HBAs- and AS-added formulations as compared to formulations containing only HBAs or AS. This may be due to the apparent higher rubbery modulus, since higher photopolymerization conversion of the acrylate functional groups on HBAs and AS is less possible due to early vitrification in these formulations.[20,27]

Thermal stability of the soy-based, UV-curable coatings was studied using Thermal Gravimetric Analyzer (TGA). The percent weight loss of the samples was plotted as a function of temperature and shown in Figure 13. All the samples showed a two-step weight loss profile. The base formulation showed major thermal decomposition between 250 and 400°C, after which the sample continued to lose weight, but at a slower rate, until at around 590°C when all the residual material burned off. When 10 wt. % HBAs were added to the base formulation, the weight loss profiles showed a similar major decomposition temperature range to the base formulation, but at a slightly faster rate.

After the major decomposition, the HBA-containing formulations exhibited slower decomposition rate versus the base formulation, with more (about 5 wt. %) material left at the end of the TGA run. For 20 wt. % AS (AS6h or AS12h) and 10 wt. % HBAs (A8 or A18) added to the base formulation, the major decomposition event started at a lower temperature (around 200°C) and the decomposition rate was much faster than other formulations without AS before 350°C. This is due to the presence of sucrose in crosslinked networks, which starts thermal decomposition at ~186°C and shows major weight loss at maximum rate between 233°C and 300°C.[34] After ~350°C, the AS-added formulations decomposed at a slower rate than the formulations without AS. Solid char formation as a result of the degradation of the sucrose components may be the reason for the slower rate of weight loss observed.[34]

The biorenewable content calculated in % wt. for the raw materials is 80%, 60%, 53% and 55% for ASO, ATHF,

FIGURE 14

Biorenewable content in % wt. for the formulations studied
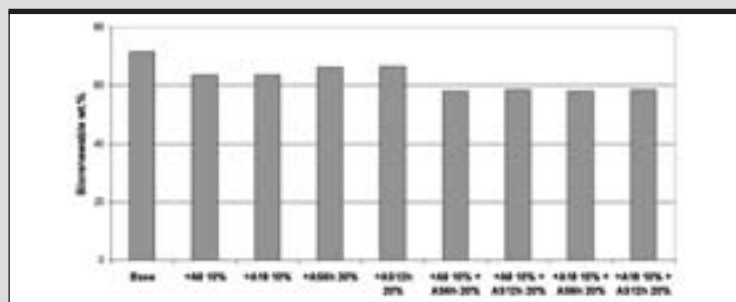
AS6h and AS12h, respectively. The biorenewable content calculated for the soy-based, UV-curable coating formulations studied is shown in Figure 14. Acrylic acid is not counted as a bio-derived chemical in the calculations. When combining the HBAs and "sweet" AS as reactive toughening agents into the base formulation, the biorenewable content of the modified formulations decreased by ~10-15% wt. to ~55-60% wt., which is still reasonably high. On the other hand, the coating performance increased significantly, owing to the unique structural features of the HBAs and the AS discussed previously. Thus, the feasibility of producing soy-based, high-performance, UV-curable coatings with high biorenewable content is demonstrated.

Conclusions

Acrylated sucrose oligomers were synthesized and characterized using mass spectroscopy and FTIR. AS oligomers had good solubility in common organic solvents and acrylate reactive diluents. Acrylate functionality of AS increased with reaction time. The addition of higher Tg, polyester HBAs into the ASO-based, UV-curable formulations increased the coating mechanical properties as well as glass transition temperature and tensile modulus, but decreased the crosslink density and tensile elongation. Addition of the "sweet" AS significantly enhanced the coating impact resistance and tensile elongation, which was attributed to the microphase separation in the crosslinked coating films and the tougher structure of AS. A high level of AS in the formulations resulted in high coating hydrophilicity and film delamination during water immersion. The combination of HBAs and AS in the ASO-based, UV-curable formulations produced "green" coatings containing ~60% wt. biorenewable ingredients with much enhanced and balanced coating properties. ❯

References

1. Rajni HK, Törnvall U, Gustafsson L, Börjesson P, Trends in Biotechnology 2007, 25, 119-124.

2. The Plant Journal 2008, 54, 536-545.

3. Wicks ZW, Jones FN, Pappas SP, Wicks DA, Organic coatings: science and technology; Third Edition ed.; A John Wiley & Sons Inc., Publication: Hoboken, New Jersey, 2007.

4. Joshi R, Provder T, Kustron K, JCT CoatingsTech 2008 5, 38-43.

5. Orr L, Paints & Coatings, "A Market Opportunity Study Update," Omni Tech International, Ltd., 2009. http://www.soynewuses.org/downloads/Mo_Paints_and_Coatings.pdf.

6. Chen ZG, Chisholm BJ, Kim JS, Stafslien SJ, Wagner R, Patel S, Daniels JW, Vander Wal L, Li J, Ward K, Callow M, Thompson S, Siripirom C, Polymer International 2008, 57, 879-886.

7. Radtech Technical Committee, "UV/EB Technology, A Way to Reduce Greenhouse Gas Emissions," Radtech Report 2005; Vol. May/June.

8. Golden R, "Low-Emission Technologies: A Path to Greener Industry," Radtech Report 2005, May/June.

9. Burak L. Journal of Coatings Technology 1997, 69, 29-32.

10. Petersen K, Nielsen PV, Bertelsen G, Lawther M, Olsen MB, Nilssonk NH, Mortenseny G, Trends in Food Science & Technology 1999, 10, 52-68.

11. Demirbas A, Biofuels, Securing the Planet's Future Energy Needs; Springer London, 2009.

12. United Soybean Board, "Technical Data Review: Soy-Based Paints and Coatings," 2009. http://www.soynewuses.org/downloads/Tech_Paints.pdf.

13. Teng GH, Soucek MD, Macromol. Mater. Eng. 2003, 288, 844-851.

14. Shi WF, Jiang Y, Liu HW, Journal of photopolymer science and technology 1992, 5, 453-459.

15. Zhu PK, X. J., Zuobang Li Hebei Gong xueyuan Xuebao 1992, 21, 8-18.

16. Cai J, Shu WB, Yun LG, Jiu LH, Tuliao Gongye 2006, 36, 12-15.

17. Gu H, Ren KT, Dustin M, Thomas M, Douglas NC, Journal of Coatings Technology 2002, 74, 49-52.

18. Ramya R, Greg S, Jamil B, Massingill J, RadTech Report, 1998, 12 36-40.

19. Sharma V, Kundu PP, Prog. Polym. Sci. 31 2006. 983–1008 2006, 31, 983-1008.

20. Shi WF, Jiang Y, Liu HW, Trends in Photochemistry and Photobiology 2001, 7, 131-144.

21. Joachim K, Thomas O, Germany Patent Application 1995; DE 1995-19545870, p 6.

22. Patil NS, Li YZ, Rethwisch DG, Dordick JS, Journal of Polymer Science, Part A: Polymer Chemistry 1997, 35, 2221-2229.

23. Ebert J, "Furfural: Future Feedstock for Fuels and Chemicals," Biomass Magazine Sept. 2008. http://ethanolproducer.com/article.jsp?article_id=4872.

24. Kamel C, Bernard B, Ghislain D, Shane S, Ce'dric L, Journal of Polymer Science: Part A: Polymer Chemistry, 2008, 46, 7972-7984.

25. Mathlouthi M, Reiser P, Sucrose: Properties and Applications; Blackie Adademic and Professional: Glasgow, 1994.

26. Grundmeier G, Stratmann M, Annu. Rev. Mater. Res. 2005, 35, 571-615.

27. Chen ZG, Webster DC, Polymer 2006, 47 3715-3726.

28. Lee DK, Tsai HB, Standford JL, Journal of Polymer Research 1996, 3, 159-163.

29. Zheng JR, Ozisika R, Siegela RW, Polymer 2006, 47, 7786-7794.

30. Chattopadhyay DK, Sreedhar B, Raju KVSN, Ind. Eng. Chem. Res. 2005, 44, 1772-1779.

31. Miller JA, Lin SB, Kirk KS, Hwang KS, Wu P, Gibson E. Cooper SL, Macromolecules 1985, 18, 32-44.

32. Sharma V, Kundu PP,. Biomacromolecules 2007, 8, 2476-2484.

33. Pettersson B, "Hyperbranched Polymers—Unique Design Tools for Multi Porperty Control in Resins and Coatings," http://www.perstorp.com/upload/hyperbranched_polymers.pdf.

34. Richard GN, ShaJzadeh F, Aust. J. Chem. 1978, 31, 1825-1832.

—Zhigang Chen, Jennifer F. Wu, Shashi Fernando, Katie Jagodzinski are associated with the Center for Nanoscale Science and Engineering at North Dakota State University, in Fargo, N.D.